Exploring Bikaverin as Metal ion Biosensor: A Computational approach.

Zakir Hussain¹, Haamid R. Bhat², Tahira Naqvi³, Malay K. Rana², Masood Ahmad Rizvi^{1*}

¹Department of Chemistry, University of Kashmir, Hazratbal, Srinagar J&K, India.

²Department of Chemical Sciences, IISER, Berhampur, Odisha, India.

³ Department of Chemistry, Degree College for Women M.A. Road Srinagar J&K, India

Corresponding Author: (Masood Ahmad Rizvi; masoodku2@gmail.com)

Abstract

A computational exploration of fungi produced pigment bikaverin as a biosensor towards bioavailable metal ions is presented. Systematic studies of the optimized ground and excited state geometries were attempted for exploring metal ion binding pocket, comparative binding propensity and optical properties of the bikaverin and its adducts with studied metal ions. The screening of 13 bioavailable metal ions, revealed a range of binding strength towards bikaverin receptor with Ca^{2+} , Mg^{2+} and Al^{3+} as the strongest binders. Besides, upon binding to bikaverin receptor an enhancement in its fluorescence intensity was observed in the order Ca^{2+} > Al^{3+} > Mg^{2+} . The computationally predicted selectivity of bikaverin receptor towards Ca^{2+} was experimentally corroborated through the preliminary fluorescence studies. The bikaverin probe showed an enhancement of fluorescence emission in presence of Ca^{2+} ions in buffered aqueous medium.

Keywords: Computational chemistry, Biosensors, Fluorescence Spectroscopy, Quantum chemical calculations, Electronic structure.

Introduction

1 2 3

4

5

6

7

8

9

10

11

12

13

14

15

16

17

18

19

20

21

22

23

24

25

26

27

28

The well designed computational studies can be good to predict the starting point for targeted experiments in a time and cost effective manner.^{1,2} Experimental chemists use theoretical calculations to supplement, support and guide their experiments particularly in the areas of conformational analysis,³ reaction mechanism,⁴ transition states,⁵ charge distributions,⁶ modeling larger molecules like DNA and proteins, ⁷ structure-activity relationships, ⁸ orbital interactions,9 and excited state studies. Metal ions are required for a plethora of functions in biosystems. However, the metal ions can be like double-edged swords; at their selected concentrations these remain coordinated to their natural binding sites performing the desired job. A change in their concentration can lead to their de-compartmentalization bringing onset of deleterious functions. 10 Therefore, selective sensors for detection and quantification of metal ions for their real time analytical monitoring and medical diagnosis are of considerable importance. ¹¹Consequently, it becomes imperative to investigate the natural bioactive compounds for their in vivo metal ion sensing applications in order to potentiate the therapeutics. In continuation of our interests in investigating the bioactivities of natural products, 12-15 we attempted to survey the fluorescent fungi derived bioactive natural product bikaverin for metal ion sensing ability. Bikaverin is a reddish pigment produced by different fungal species of the genus Fusarium with the diverse biological activities. 16-18 With the increasing reports on its pharmacological role, bikaverin is becoming a metabolite of increasing biotechnological interest.¹⁹ Commercially bikaverin as pure compound is costly and synthesizing bikaverin through a total chemical process is less viable and environmentally unfavorable. However, obtaining bikaverin from microbial sources presents an environment friendly and continuous source. Thus for obtaining bikaverin in a cost effective and an environment friendly manner, we extracted bikaverin from fungal extracts under the standardized literature reports.²⁰ In this study, we present the computational exploration of bikaverin as biosensor towards thirteen bioavailable metal ions. The computational prediction was experimentally confirmed through initial florescence studies of studied metal ions as bikaverin adducts.

293031

Experimental

32 33

Computational procedures and materials

34 35

36

All the density functional theory (DFT) and time-dependent density functional theory (TD-DFT)

calculations were performed using the Gaussian 09 program package. The geometries of

1 all the molecules with and without metals were fully optimized at the singlet ground (S₀) and first 2 excited (S1) states in the acetonitrile solvent using CAM-B3LYP, Coulomb-attenuating method 3 based on Becke's three parameter hybrid exchange and nonlocal correlation functional of Lee, 4 Yang and Parr (65% exchange and 35% correlation weighting at long-range). 21,22 The standard 6-5 311G, split-valence atomic basis setfunction of DFT has been employed for all the atoms except 6 for the transition metals, Nickel (Ni²⁺), Mercury (Hg²⁺), Cadmium (Cd²⁺), Manganese(Mn²⁺), 7 Iron (Fe²⁺), Zinc(Zn²⁺), Copper(Cu²⁺) and Lead (Pb²⁺) atoms for which effective core potential 8 (ECP) of Wadt and Hay pseudo-potential with a double-ζ valence basis set LANL2DZ was used. 9 ²³⁻²⁵ It is because the LANL2DZ reduces the computational cost as it uses an effective core 10 potential for the core electrons, thus the core electrons are not explicitly considered in the 11 computation. For the structural calculations of receptor-transition metal complexes, the 12 13 relativistic LANL2DZ pseudopotential is the typical basis set and is identified to give close agreement between calculated and experimentally observed geometries. Frequency calculations 14 were carried out to verify that the optimized molecular structures correspond to the energy 15 16 minima, thus only positive frequencies were expected. The TD-DFT studies of all the molecules were performed by utilizing the same functional and the basis sets as CAM-B3LYP has been 17 shown to be good for the excited state property calculations. ^{26,27} The Conductor-like Polarizable 18 Continuum Model (CPCM) was utilized for taking care of the effect of solvation in acetonitrile 19 (dielectric constant, $\varepsilon = 37.5$) on all the calculations as implemented in Gaussian 09. Natural 20 Bond Orbital (NBO) method was exploited for the natural population analysis, using the NBO 3.1 21 version as implemented in Gaussian 09 program.²⁸ Free energy changes (ΔG) and binding 22 energies (ΔE) were calculated for the receptor-analyte complexes to comprehend the 23 thermodynamic binding propensity of the selected bioavailable cations with receptor (1). The 24 Gibbs free energy change (ΔG) of the fragments (1), Na⁺, K⁺, Ni²⁺, Al³⁺, Hg²⁺, Cd²⁺, Mn²⁺, 25 Fe²⁺, Zn²⁺, Cu²⁺, Mg²⁺, Fe³⁺, Pb²⁺ and Ca²⁺ and their complexes were calculated following the 26 27 equation 1: 28 (1) $\Delta G = G_{complex} - (G_{receptor} + G_{cation})$

29

- Where (Gcomplex) is the free energy of receptor-cation adduct, Greceptor and Gcation are free 30
- energies of isolated receptor and cation respectively. The binding energy changes were also 31
- calculated to check the binding selectivity of the studied cations towards bikaverin 32
- receptor following the equation 2: 33

34 (2) $\Delta E = (E_{complex}) - (E_{receptor} + E_{cation})$ 35

Where Ecomplex is the total energy of the receptor-cation adduct, Ereceptorand Ecation are total 36

energies of isolated receptor and cation respectively. In order to reduce basis set superposition error (BSSE) in these energy calculations, the Boys-Bernardi scheme was applied to yield the counterpoise corrected energies. ²⁹

Extraction of Bikaverin from Fungal Extracts:

Fungal mycelium showed a growth up to 5-6 cm on a PDA (potato dextrose agar) plate after 7 days. The morphological features supported the genus *Fusarium* resulting in 99 % homology with the *Fusarium proliferatum*. Dichloromethane solvent was used to extract the crude bikaverin using National Cancer Institute's protocol. The extract was concentrated under vacuum and subjected to purification over column chromatography on silica gel using hexane-ethyl acetate (7:3 V:V) mobile phase leading to the isolation of pure bikaverin.

Absorption and emission studies

All reagents were purchased from Aldrich and used without further purification. UV-Vis and fluorescence spectra were recorded on a Shimadzu UV-2450 and Shimadzu 5301 PC spectrophotometer respectively, with a quartz cuvette (path length 1 cm). A 10^{-3} M stock solution of bikaverin (probe 1) was prepared by dissolving the required amount of bikaverin in 10 mL of DMSO; 30μ L of this stock solution was further diluted with CH₃CN and HEPES buffer (0.05 M, pH = 7.4) to prepare 3 mL solution of probe (1) and this solution was used for each UV–Vis and fluorescence experiment. The aliquots of freshly prepared standard solutions (10^{-2} M) of metal chloride/metal perchlorates{M = Hg²⁺, Fe²⁺, Fe³⁺, Pb²⁺, Cd²⁺, Cu²⁺, Zn²⁺, Ni²⁺, Al³⁺, Co²⁺, Mg²⁺, Ca²⁺, Na⁺, and K⁺}, in distilled water were added to 3 mL solution of probe (1) taken in quartz cuvette and spectra's were recorded.

Results and discussions

Quantum-chemical calculations are impressive for their step to step analysis and prediction whereas experimental results are a net outcome of all the influencing factors in a blend.³⁰ The natural charge distribution (Table 1) and electrostatic potential map of bikaverin (1) were calculated to identify its appropriate cation binding site. The data in Table 1 and electrostatic potential map of bikaverin (1) indicate that the pocket for the electrophilic addition of cations is the carbonyl and the hydroxyl oxygen atoms Fig 1 (ground state structure of bikaverin).

Fig 1. Optimized geometry and Electrostatic potential map of Bikaverin **S**₀ ground state. **Table 1**: The NPA Charge distribution on some crucial atoms of bikaverin **1** and **1-Ca**²⁺ in **S**₀ calculated at CAM-B3LYP/6-311G level of theory.

Atom involved	NPA charge distribution		
Atom mvorveu	Bikaverin (1)	1-Ca ²⁺	
O22	-0.685	-0.776	
O19	-0.534	-0.678	
O23	-0.645	-0.635	
O21	-0.698	-0.685	
O20	-0.588	-0.559	
O24	-0.495	-0.495	
O25	-0.532	-0.527	
O26	-0.516	-0.513	
H36	-0.523	-0.551	
Ca43		1964	

The optimized geometries and the corresponding energies of the ground and first excited state of bikaverin(1) and its receptor-analyte complexes with thirteen(13) studied bioavailable metal ions are shown in Fig. 2 and S1 and S2 respectively (See Supplementary information). The calculated free energy change (ΔG) and the binding energy (ΔE) values of receptor analyte complexes are presented in Table 2. The data in the Table 2 reveals that the binding of all the cations is thermodynamically feasible and studied bioavailable metal ions bind the bikaverin receptor (1) with a range of strength. The trend in the binding propensity of studied metal ions can be correlated to their charge densities and hard soft acid base strength. It is evident from the binding and free energy data of Table 2 that the electrophillic binding of Ca²⁺, Mg²⁺ and

Al³⁺ with receptor (1) is stronger in comparison to the other studied metal ion cations. Among all the studied metal ions the binding of Ca²⁺was found to be strongest which suggests a possible sensing ability of the bikaverin receptor (1) towards Ca²⁺ ions at their physiological concentrations.

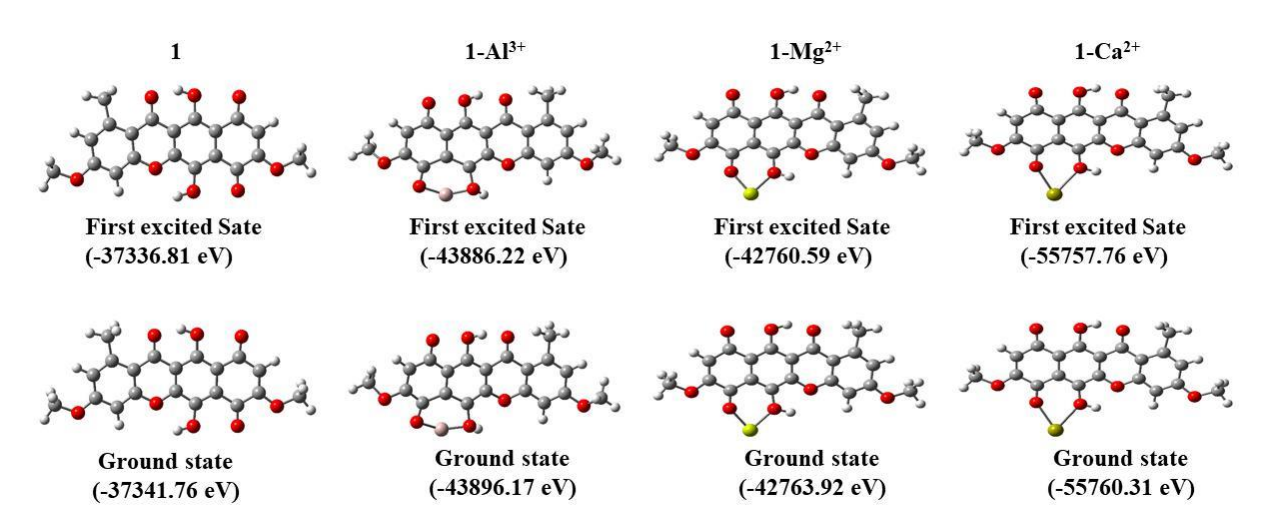


Fig 2. Optimized ground (S₀) and the first excited state (S₁) geometries of bikaverin receptor(1),1-Al³⁺, 1-Mg²⁺ and 1-Ca²⁺ and their corresponding energies [in electron volts (eV)].

Motivated by the binding of metal ions to bikaverin (1) receptor, we attempted to explore the fluorescence behavior of the studied metal ions for possible sensing applications. To get an insight into the origin of absorption and emission bands, the transitions of the bikaverin(1) and its receptor-analyte complexes under consideration were simulated using the selected DFT/TD-DFT level of theory (Experimental section). The calculated spectras of the studied metal ion bikaverin (1) adducts determined in the acetonitrile solvent depicted various peaks. However only the peaks of highest intensity fluorescence were preferred for analysis. The major absorption and fluorescence intensity band of bikaverin (1) and its receptor-analyte adducts with studied metal ions are summarized in Table 3. The calculated absorption spectrumfor bikaverin (1) shows a major peak(λ_{abs}) at 491 nm (2.52 eV). The metal ion bikaverin adducts showed varied emission responses in which the fluorescence intensities in some cases were seen to be attenuated and in some cases enhanced. The calculated fluorescence intensities of 1-Ca²⁺,1-Mg²⁺ and 1-Al³⁺adducts were found to be significantly higher than that of bikaverin (1) while as the absorption intensities of their receptor-analyte complexes don't show much deviation in comparison to pure bikaverin (1).

Table 2: Calculated free energy change (ΔG) and binding energy for receptor-analyte complexes using CAM-B3LYP/6-311Glevel of theory with basis set superposition error (BSSE) corrections.

S. No	Fragment	ΔG (Kcal/mol)	Binding energy (Kcal/mol)	S. N o	Fragment	ΔG (Kcal/mol)	Binding energy (Kcal/mol)
01	(1)	-29.52	-	08	1-Zn ²⁺	-31.66	-23.77
02	1-Na ⁺	-22.44	-41.94	09	1-Mn ²⁺	-43.76	-31.81
03	1-K ⁺	-19.92	-39.31	10	1-Fe ²⁺	-55.39	-50.11
04	1-Al ³⁺	-53.09	-52.96	11	1-Ni ²⁺	-27.11	-29.72
05	1-Pb ²⁺	-51.31	-22.72	12	1-Cu ²⁺	-34.64	-39.94
06	$1-Hg^{2+}$	-15.29	-34.20	13	$1-Mg^{2+}$	-51.97	-58.63
07	1-Cd ²⁺	-22.64	-45.29	14	1-Ca ²⁺	-73.19	-69.21

To have a further insight into the emission behavior of the bikaverin (1) metal ion adducts, the frontier molecular orbitals (FMOs) analysis was attempted. The FMOs of the bikaverin (1) and some representative receptor-analyte complexes are depicted in Fig. 3. The highest occupied molecular orbital (HOMO) and lowest unoccupied molecular orbitals (LUMO) energies of bikaverin (1) and all its metal ion adducts have been summarized in (Table S1, see supporting information). The interactions between the metal ions and the bikaverin (1) can be clearly observed from the frontier molecular orbital contour distribution. In case of bikaverin (1), the HOMO and LUMO are spread evenly over the benzoquinone and hydroquinone rings of the molecule. The observed changes in the HOMO and LUMO contours of bikaverin (1) indicate a pi to pi* transition in absorption. However, HOMOs and LUMOs in the receptor-analyte adducts are budged on different regions of the adducts indicating intramoleculor charge transfer due to the binding of cationic species 32,33

Table 3: Summary of absorption and fluorescence spectral data of bikaverin(1) and its analyte complexes

1
2
3
4
5
1 2 3 4 5 6 7 8 9
7
8 9 10 11 12
10
10
11
13
14
15
16
17
18
19
20
21
12 13 14 15 16 17 18 19 20 21 22 23 24 25
23 21
25
23

Molecule	Calculated	Oscillator strength	Calculated	Oscillator strength	
	$\lambda_{abs}(nm)$	(f)	λflu(nm)	(f)	
1	491	0.2524	576	0.0102	
1-Na ⁺	412	0.1960	426	0.0081	
1-K ⁺	315	0.1910	370	0.0013	
1-Ni ²⁺	441	0.2103	494	0.0014	
1-Al ³⁺	342	0.1543	388	0.1976	
$1-\mathrm{Hg}^{2+}$	377	0.1130	435	0.0045	
1 -Cd $^{2+}$	389	0.1866	437	0.0043	
1-Mn ²⁺	422	0.2010	497	0.0036	
1-Fe ²⁺	360	0.2349	454	0.0045	
1-Zn ²⁺	390	0.1873	437	0.0033	
1-Cu ²⁺	391	0.1033	463	0.0002	
$1-Mg^{2+}$	372	0.1537	422	0.1278	
1-Pb ²⁺	418	0.1004	471	0.0037	
1-Ca ²⁺	525	0.1629	588	0.3722	

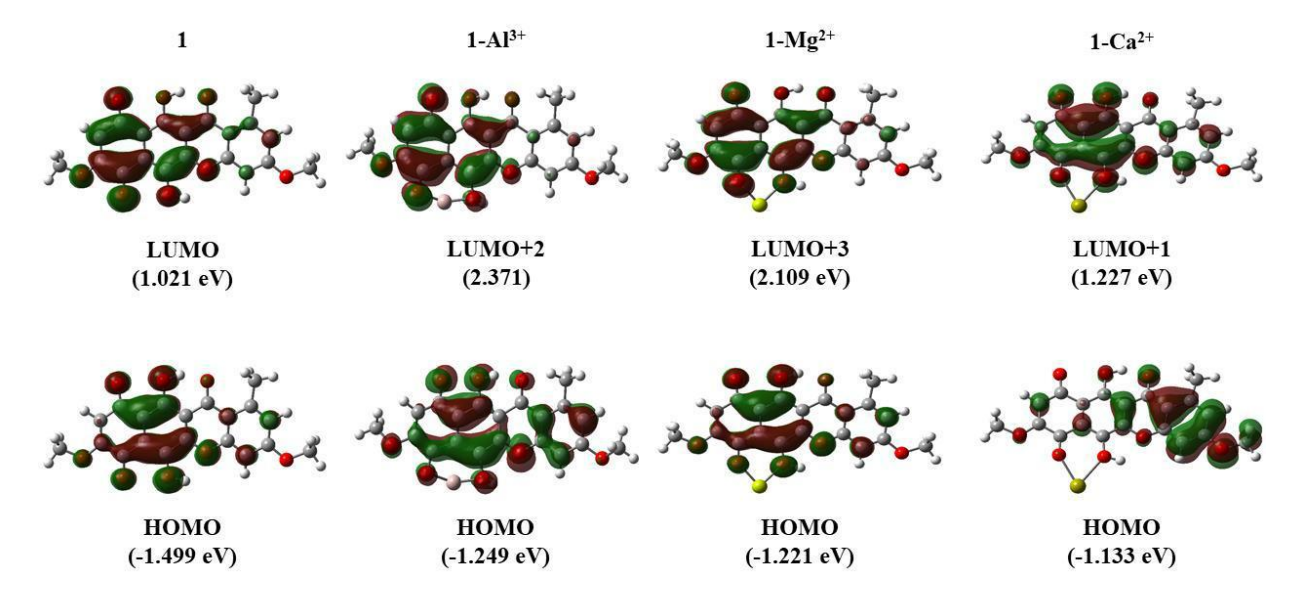


Fig 3:Frontier molecular orbitals of bikaverin (1), 1-Al³⁺, 1-Mg²⁺ and 1-Ca²⁺.

1 2 It can also be seen from the Fig. 3 that the orbital contour distribution of HOMO in case of bikaverin calcium ion adduct (1-Ca²⁺) gets shifted towards the opposite end compared to free 3 bikaverin (1) or 1-Al³⁺ and 1-Mg²⁺ adducts. The calculated fluorescence wavelength for 4 bikaverin (1) was found to be 576 nm (2.15 eV) with oscillator strength of 0.0102, depicting 5 low intensity fluorescence peak in bikaverin (1). While the calculated fluorescence spectrum 6 of 1- Ca^{2+} shows an intense peak at 588 nm (2.19 eV) with oscillator strength of 0.3722. 7 8 Thus the observations of strong Ca²⁺ ion binding coupled with the enhancement in the 9 fluorescence intensity of bikaverin (1) on Ca²⁺ ion binding predict the bikaverin (1) as the new 10 possible fluorescent biosensor for Ca²⁺ ion. The fluorescence imaging of Ca²⁺ ions in the form 11 of bikaverin (1) calcium adduct can serve as a method for analyzing signaling pathways involving 12 calcium ions. Besides, the changes in the intracellular Ca²⁺ ion concentrations have been related 13 to different physiological, pathological and immune responses, therefore bikaverin based calcium 14 ion sensing can also be important in diagnostics. The calculated oscillator strengths of fluorescence intensities of studied bioactive metal ions with 17 bikaverin (1) also predict a mild to medium increase in the intensity in case of 1-Mg^{2+} and 1-18 Al³⁺adducts. But the intensities of their fluorescence peaks are predicted to be smaller in 19 comparison to Ca^{2+} as depicted by their oscillator strengths of 0.1976 and 0.1278, respectively. 20 For the other cationic species, there is no significant effect on the fluorescence intensities once 21 22 23 they bind with the bikaverin receptor (1) as can be seen from their oscillator strengths in Table 24 25 3. It is therefore predicted from the DFT/TD-DFT calculations that receptor (1) can strongly sense Ca^{2+} ions fluorometrically with the milder sensing ability towards Mg^{2+} and Al^{3+} 26 among the studied bioactive metal ions. The probable reason for the fluorescence intensity 27 28 enhancement in case of 1-Ca²⁺, 1-Al³⁺, and 1-Mg²⁺ adducts is that their absorption transitions 29 involve electron shifting to higher singlet excited states like fourth singlet excited state (S4), 30 31 third singlet excited state(S₃) and second singlet excited state(S₂) in case of 1-Ca²⁺, 1-Al³⁺, and 32 1-Mg²⁺ respectively. As per Kasha's rule, the fluorescence phenomenon occurs from the first 33 34 singlet excited state (S1).34 In order for fluorescence to occur, the higher excited states have to 35 relax to the first singlet excited state. For this relaxation process, internal conversions and the 36 vibrational relaxations occur which lead to the loss of energy during the de-excitation. Due to this 37 energy loss there is significant Stoke's shift (change between absorption and emission energies) 38 leading to occurrence of fluorescence and its intensity enhancement. While as in the other cations 39 and in receptor (1), the transitions involve the lowest singlet excited state S₁. So there is no 40 internal conversion and hence no energy loss and eventually no Stoke's shift. Hence, in such 41 cases, there is either no fluorescence or the intensity of the fluorescence is very weak. 42

TD-DFT calculated results show that the main transitions for bikaverin(1), 1-Al³⁺, 1-Mg²⁺and1-Ca²⁺are from HOMO→LUMO, HOMO→LUMO+2, HOMO→LUMO+3and HOMO→LUMO+1 respectively see Fig 4. In all other receptor-analyte complexes, the main transitions involve HOMO→LUMO.

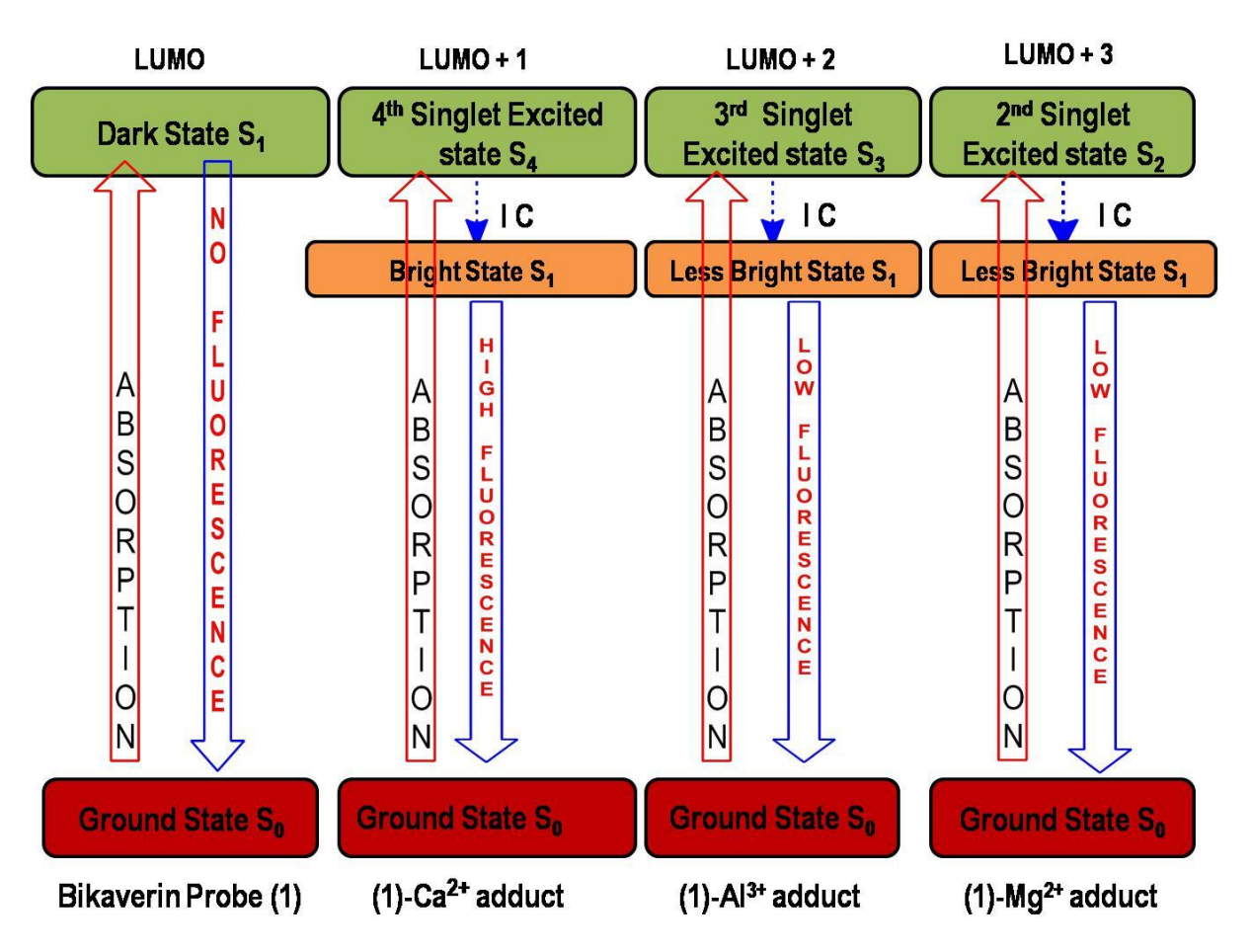


Fig 4. Predicted electronic excitations and de excitations of bikaverin receptor (1) and its calcium adduct

Characterization of Bikaverin from Fungal Extract:

The developments in synthetic biology has allowed tuning of microbial systems for generating industrially viable strains as the green and sustainable sources of value-added compounds.³⁵The composition and amounts of metabolites(bikaverin) are specific to the species of genus Fusarium. The morphological features of our crude fungal extract matched to the species *Fusarium proliferatum* see Fig 5.

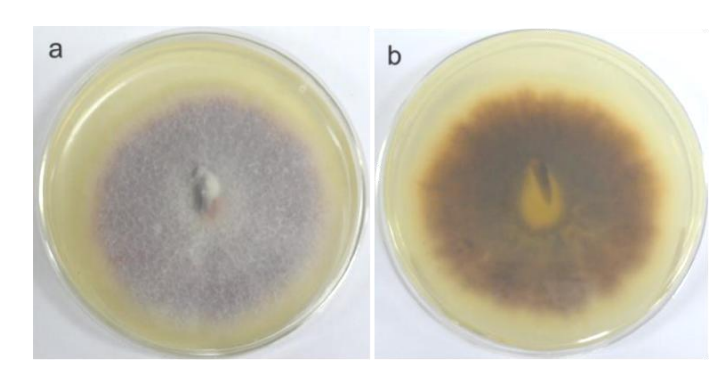


Fig 5:Morphological feature of *Fusarium proliferatum*a,b the obverse (a) and reverse (b) view of mycelium.

The chemical structure of purified bikaverin was confirmed through comparative analysis of NMR, mass, λ max and TLC of isolated compound with bikaverin standard and further to the literature reported values.³⁶¹H-NMR (CDCl₃, 400MHZ): δ 2.87 (3H, s, 1-Me), 3.93 (3H, s, 8-OMe), 3.96 (3H, s, 3-OMe), 6.35 (1H, s, H-9), 6.81 (1H, s, H-2), 6.93 (1H, s, H-4).HRMS (ESI⁺) calculated for C₂₀H₁₄O₈ [M+H]⁺: 381.0761, found: 382.90 Fig.6.

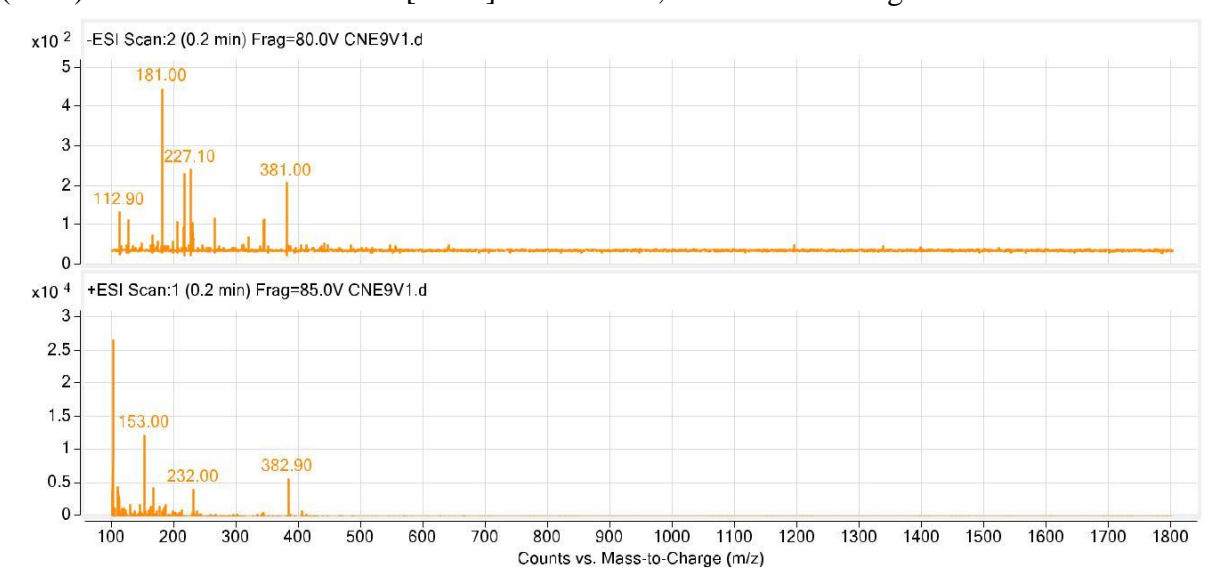
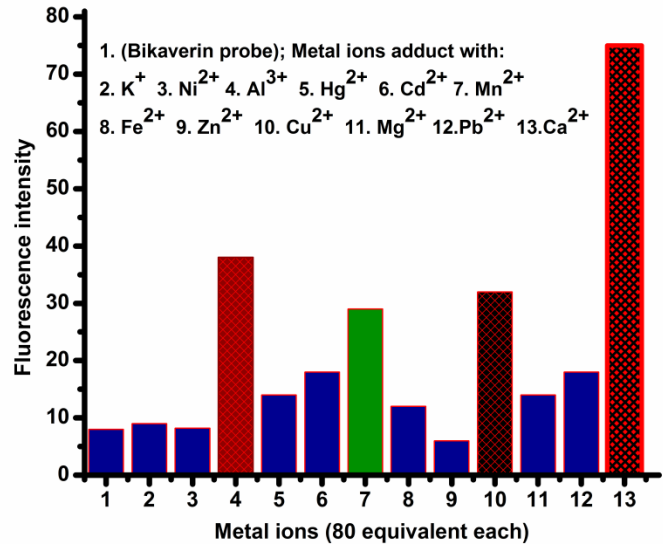


Fig. 6. Mass spectra of isolated product Bikaverin

Metal ion sensing Applications

The preliminary metal ion sensing behavior of bikaverin (1) was studied towards selected bioactive metal ions as their chloride/perchlorate salts in CH₃CN/H₂O (6:4, v/v; buffered with PBS, pH 7.4) using fluorescence spectroscopy Fig 7.The fluorescence spectrum of receptor (1) (10.0 μ M) exhibits a weak emission band at 620 nm corresponding to bikaverin moiety when excited at 596 nm in CH₃CN/H₂O (6:4, v/v; buffered with PBS, pH=7.4). The weak

fluorescence emission behavior of bikaverin is due to intramolecular charge transfer process as seen from HOMO- LUMO orbital contours.



9

Fig. 7.Fluorescence response of bikaverin(1)towards various metal ions: Bars represent fluorescence selectivity (I/Io) of bikaverin (1) (10.0 μ M) towards various metal ions(80 equiv each) in CH₃CN:H₂O (6:4, v/v) buffered with 0.05 M HEPES, pH = 7.4; λ ex = 596 nm. The experimental fluorescence spectra of bikaverin(1) and its calcium adduct under different excitation wavelengths are shown in Fig.8 (A,B) respectively.

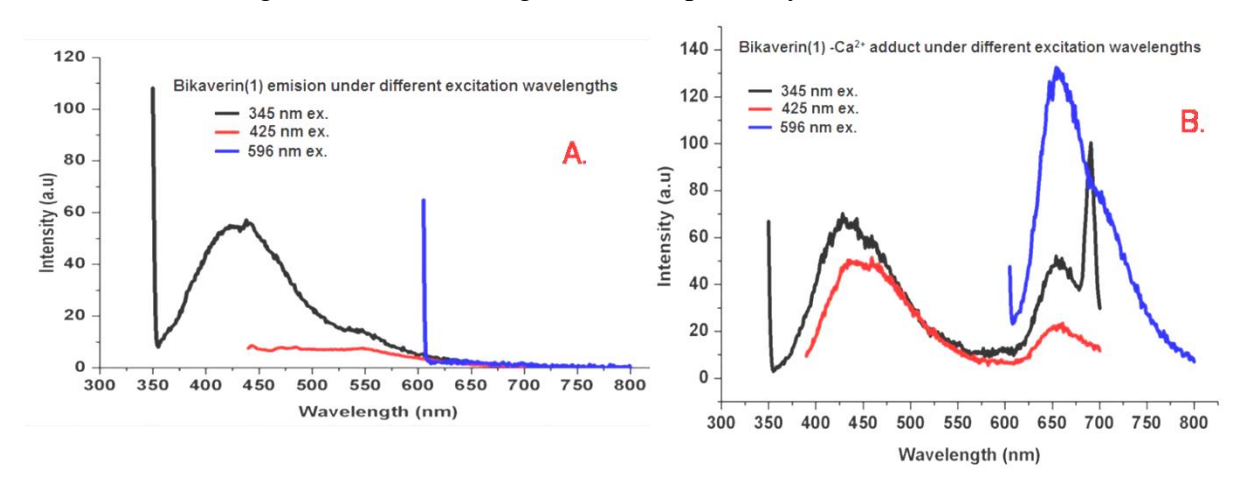


Fig. 8.Fluorescence response under different excitation wavelengths for A: bikaverin(1) B: Bikaverin Ca²⁺ adduct.

It is evident from figure 8 that on binding of calcium ions to bikaverin (1) its fluorescence profile gets modified. The free bikaverin shows very little to no fluorescence when excited at 596 nm while as the calcium bound bikaverin shows a major fluorescence when excited at the 596 nm wavelength. Among the fluorescence peaks obtained under the excitation

- wavelengths of 425 and 345 nm, the former gets an enhancement in the emission intensity 1
- while as the latter peak remains largely unchanged on calcium ion binding to bikaverin. 2

Conclusions

3 4 In summary, the present work describes a thorough computational investigation of metal ion 5 sensing ability of natural pigment bikaverin as a fluorescent probe. An exploration of 6 comparative metal ion binding affinities and optical properties of the bikaverin adducts through 7 systematic studies using the appropriate level of theory are presented. The Ca^{2+} , Mg^{2+} and Al^{3+} 8 metal ions are shown to bind the bikaverin receptor more strongly and with an enhancement in its 9 florescence intensity. The strongest binding affinity with the most intense fluorescence emission 10 in case of Ca²⁺predicts bikaverin pigment as a possible Ca²⁺biosensor. The concept of isolation 11 of bikaverin receptor (1) from the natural source as an economical and sustainable method is also 12 presented. The computationally predicted metal ion fluorescence behavior of bikaverin receptor 13 (1) towards the studied metal ions was experimentally corroborated through the preliminary 14 fluorescence studies. Among the studied metal ions, the bikaverin receptor (1) was seen to 15 strongly detect Ca²⁺ions with an enhancement of fluorescence emission in its µM concentration 16 range in the buffered aqueous medium due to charge transfer phenomena. The inclusive 17 experimental studies of the bikaverin receptor (1) towards the selective calcium ion sensing under 18 physiological conditions, the complete analytical profile of bikaverin as biosensor, the real time 19 imaging of Ca²⁺ions in cells through confocal microscopy and other related studies for the 20 buildup of bikaverin as Ca²⁺ion biosensor are underway in our laboratory. 21

22

23 24

Acknowledgement

- MAR thankfully acknowledges Dr Hemant J Purohit, Chief Scientist & Head Environmental 25
- Genomics Division, National Environmental Engineering Research Institute (NEERI), CSIR, 26
- Nagpur India for providing the Bikaverin crude extract for bikaverin extraction and 27
- University of Kashmir for assistance under UGC 12th innovative research activity.HRB and 28
- MKR are highly thankful to Indian Institute of Technology Kanpur, India for providing some 29
- computational facilities. 30

31 32 33

Conflict of Interest

All the authors declare no conflict of interest what so ever. 34

```
1
2
```

References:

3 4

5 1. M.A.Rizvi, M.Mane, M.A.Khuroo, G. M. Peerzada, *MonatshChem.* **2017**,*148*, 655–668.

6

7 2. Y. Dangat, M. A. Rizvi, P. Pandey, K. Vanka, *J OrganometChem.* **2016**, *801*, 30-41.

8

- 9 3. S. Krishnamurty, M. Stefanov, T. Mineva, S. Bégu, J. M. Devoisselle, A. Goursot, R. Zhu,
- 10 D. R. Salahub, J. Phys. Chem. B. **2008**,112,13433–13442.
- 4. M. Kumar, A. Kumar, M. Rizvi, M. Mane, K.Vanka, S. C. Taneja, B. A. Shah, Eur. J.
- 12 Org. Chem. **2014**, 2014, 5247–5255

13

5. M.V. Mane, M.A.Rizvi, K.Vanka, *J. Org. Chem.* **2015**, *80*, 2081–2091.

15

6. A.T. Castro, J.D. Figuero-Villar, Int. J. Quantum Chem. 2002, 89,135–146

17

- 7. M. Lintuluoto, J. M. Lintuluoto, *Biochemistry*. **2016**, *55*, 4697–4707
- 8. S. Arulmozhiraja, M. Morita, *Chem. Res. Toxicol.* **2004,** *17*, 348–356
- 9. N. Yasarawan, K. Thipyapong, V. Ruangpornvisuti, J. Mol. Graphics Model. 2014,51,13-
- 21 26
- 22 10. F. Senn, M. Krykunov, J. Phys. Chem. A. 2015, 119, 10575–10581.
- 11. M.H. Bridge, E.Williams, M.E.G. Lyons, K.F. Tipton, W.Linert. *Biochim. Biophys. Acta.*
- **24 2004,** *1690*, 77–84.
- 25 12. J.J. Zhang, F.F. Cheng, J.J Li, J.J. Zhu, Y. Lu, *Nano Today*. **2016**, *11*, 309–329.
- 13. J.Balan, J. Fuska, I.Kuhr, V. Kuhrova, Folia Microbiol (Praha). 1970, 15, 479-484.
- 27 14. J. Fuska, B. Proksa, A. Fuskova, *Neoplasma*. **1975**, 22,335-338.
- 15. D. Nirmaladevi, M. Venkataramana, S.Chandranayaka, A. Ramesha, N.M. Jameel,
- 29 Neuroprotective *Cell Mol.Neurobiol.* **2014,** *34*,973–985.
- 16. R. R. Ortiz, M. C.Limon, J. Avalos, *Appl. Environ. Microbiol.* **2009**, *75*,405-413.
- 17. D. Arora, N.Sharma, V. Singamaneni, V.Sharma, M.Kushwaha, V.Abrol, S.Guru, S.
- 32 Sharma, A.P. Gupta, S. Bhushan, S. Jaglan, P. Gupta, *Phytomedicine*. **2016**, 23,1312-1320.
- 18. A. D. Becke, *J. Chem. Phys.* **1993**,98,5648–5652.
- 19. C. Lee, W. Yang R. G. Parr, *Phys. Rev. B.* **1988**, *37*,785–789.
- 35 20. W. R. Wadt, P. J. Hay, J. Chem. Phys., 1985,82, 284–298.
- 21. A. Sivaramakrishna, C. Sravani, S. Venkatesh, B. B. Pavankumar, K. Vijayakrishna, H.
- 37 R. Bhat, P. C. Jha, G. S. Smith, *RSC Advances*. **2016**,*6*,105528–105539.
- 38 22.S. Venkatesh, C. Sravani, S. Janardan, P. Suman, E. V. Goud, B. B. Pavankumar,
- V.Leninkumar, H.R.Bhat, A. Sivaramakrishna, K. Vijayakrishna, P.C.Jha G. S. Smith, J.
- 40 *Organomet. Chem.* **2016,**818,72–81.
- 41 23. H. R. Bhat ,P. C. Jha, Chem. Phys. Lett. **2017**,669, 9–16.
- 42 24. H.R.Bhat, P.C.Jha, *Phys. Chem. Chem. Phys.* **2017**, *19*,14811–14820.
- 43 25. H.R.Bhat, P.C. Jha, J. Phys. Chem. A. **2017**, 121, 3757–3767.
- 44 26. A.E.Reed L.A.Curtiss, F. Weinhold, *Chem. Rev.* **1988**, 88, 899–926.
- 45 27. S.F.Boys, F. Bernardi, *Mol. Phys.* **1970**, *19*, 553–566.

- 1 28. M. A. Rizvi, M. Zaki, M. Afzal, M. Mane, M.Kumar, B. A. Shah, S.Srivastav,
- 2 S.Srikrishna, G. M. Peerzada, S. Tabassum, Eur. J. Med. Chem. 2015,90, 876-888.
- 3 29. J.W. Cornforth, G.Ryback, P.M. Robinson, D. Park, J Chem Soc Perkin 1971, 1.16,
- 4 2786-2788.
- 5 30. R. M. Jagtap, M. A. Rizvi, Y. B. Dangat, Satish K. Pardeshi, J. Sulfur Chem. 2016, 37,
- 6 401-425
- 31. J.Katla, H.R.Bhat, P.C.Jha, P.S. Ghalsasi, S Kanvah, Chemistry Select. 2017, 2, 1902–
- 8 1910.
- 9 32. H.R.Bhat, P.C.Jha, *ChemistrySelect.* **2017**, 2, 2732 2739.

- 33. S.Das, H.R.Bhat, N.Balsukuri, P.C.Jha, Y.Hisamune, M.Ishida, H.Furuta, S.Mori, I.Gupta,
- 12 *Inorg. Chem. Front.* **2017**,*4*,618–638.
- 34. M. Kasha, *Discuss. Faraday Soc.* **1950,**9,14–19.
- 14 35. J.Du, Z. Shao, H. Zhao, *J Ind Microbiol Biotechnol.* **2011,** *38*,873–890.
- 36. D. Kjaer, A. Kjaer, C. Pedersen, J.D. BuLock, J.R.Smith, J. Chem. Soc. C 1971, 0, 2792-
- 16 2797.